Predicting tree biomass growth in the temperate–boreal ecotone: Is tree size, age, competition, or climate response most important?

JANE R. FOSTER[1], ANDREW O. FINLEY[2], ANTHONY W. D'AMATO[3], JOHN B. BRADFORD[4] and SUDIPTO BANERJEE[5]

[1]*Department of Forest Resources, University of Minnesota, 115 Green Hall, 1530 Cleveland Ave. N., St. Paul, MN 55108, USA,* [2]*Department of Forestry and Geography, Michigan State University, 126 Natural Resources Building, East Lansing, MI 48824, USA,* [3]*Rubenstein School of Environment and Natural Resources, University of Vermont, 204E Aiken Center, 81 Carrigan Drive, Burlington, VT 05405, USA,* [4]*US Geological Survey - Southwest Biological Science Center, Northern Arizona University, Building 20, P.O. Box 5614, Flagstaff, AZ 86011, USA,* [5]*Department of Biostatistics, UCLA School of Public Health, Room 51-254B CHS, Los Angeles, CA 90095-1772, USA*

Abstract

As global temperatures rise, variation in annual climate is also changing, with unknown consequences for forest biomes. Growing forests have the ability to capture atmospheric CO_2 and thereby slow rising CO_2 concentrations. Forests' ongoing ability to sequester C depends on how tree communities respond to changes in climate variation. Much of what we know about tree and forest response to climate variation comes from tree-ring records. Yet typical tree-ring datasets and models do not capture the diversity of climate responses that exist within and among trees and species. We address this issue using a model that estimates individual tree response to climate variables while accounting for variation in individuals' size, age, competitive status, and spatially structured latent covariates. Our model allows for inference about variance within and among species. We quantify how variables influence aboveground biomass growth of individual trees from a representative sample of 15 northern or southern tree species growing in a transition zone between boreal and temperate biomes. Individual trees varied in their growth response to fluctuating mean annual temperature and summer moisture stress. The variation among individuals within a species was wider than mean differences among species. The effects of mean temperature and summer moisture stress interacted, such that warm years produced positive responses to summer moisture availability and cool years produced negative responses. As climate models project significant increases in annual temperatures, growth of species like *Acer saccharum*, *Quercus rubra*, and *Picea glauca* will vary more in response to summer moisture stress than in the past. The magnitude of biomass growth variation in response to annual climate was 92–95% smaller than responses to tree size and age. This means that measuring or predicting the physical structure of current and future forests could tell us more about future C dynamics than growth responses related to climate change alone.

Keywords: annual climate variation, Bayesian models, carbon sequestration, dendroecology, drought, evapotranspiration, forest biomass, spatial autocorrelation, temperature, tree growth response

Received 2 September 2015; revised version received 9 December 2015 and accepted 10 December 2015

Introduction

Tree growth is known to vary annually with fluctuations in climate. In poor growing years, little to no wood grows around the outer dimensions of a tree stem, while favorable years produce higher than average growth in all dimensions. These growth variations have implications for the global carbon (C) cycle when scaled up to populations of trees, particularly when extreme events such as droughts cause widespread perturbations that lead to decline or mortality. Growing forests are important sinks for atmospheric carbon (Pan *et al.*, 2011), which means they take up and store more C through tissue growth than they release through respiration, decay or other processes. An individual tree sequesters C by assimilating CO_2 during photosynthesis and growing structural carbohydrates that make up the wood matrix. Carbon accounts for ½ of wood mass on average (but see Thomas & Malczewski, 2007), and remains stored in wood fibers for decades to centuries until it is released back to the atmosphere through combustion or decay. Annual variation in wood growth is often the most dynamic component of the terrestrial C cycle and needs to be quantified to predict forest response, and potential feedbacks, to climate change.

Correspondence: Jane R. Foster, tel. 608-215-9957, fax 267-597-3811, e-mail: jrfoster@umn.edu

Rates of forest C accumulation may be expected to change with climate if communities of tree species respond in unison to increasing annual temperatures and growing season moisture stress. Yet communities may not respond uniformly for a number of reasons. Temperate forests are composed of many interacting species with unique life history and physiological traits that cause them to respond differently. Within species, individual differences in size, age, and competitive environment further govern climate–growth response (Martínez-Vilalta *et al.*, 2011; Zhang *et al.*, 2015). This variation among individuals and within species introduces uncertainty to projections of forest growth under climate change and remains poorly characterized (Carrer, 2011).

Forest communities and their potential for C sequestration may also be altered if climate change leads to migration of warm-adapted tree species. Species' geographic distributions reflect historical tolerances to climate, leading to predictions of large-scale migration of tree species toward the poles or higher elevations with warming temperatures (Little, 1971; Iverson & Prasad, 1998; Landscape Change Research Group, 2014), under the assumption that species are able to track their historic climate envelopes in geographic space. Zhu *et al.* (2012, 2014) demonstrated this expected migration is not yet apparent in large-scale forest inventory data and satellite data have shown examples of montane tree species shifting in directions counter to climate expectations (Foster & D'Amato, 2015). As tree migration appears to lag the velocity of climate change, relative growth rates of currently co-occurring species will remain an important driver of forest composition and C accumulation over the next 50–100 years.

Two factors have limited our understanding of the impact of climate variation on annual wood growth of forest trees: (i) Analyses often rely on suboptimal measures of growth; and (ii) inferences are often based on models fit to nonrepresentative samples of trees. First, analyses commonly rely on one-dimensional (e.g., diameter growth along a single radius) or dimensionless (e.g., standardized ring-width) indices of wood growth, rather than mass-based measures. This approach limits understanding of how tree size relates to annual growth variation. Tree growth in terms of mass (and C accumulation) increases with tree size, as recently demonstrated across a global dataset (Stephenson *et al.*, 2014). This suggests that size may mediate the effects of climate reported for dimensionless growth indices, but the importance of size relative to climate response remains unresolved (Chu *et al.*, 2015; Michaletz *et al.*, 2015).

Although these one-dimensional and dimensionless indices of wood growth can provide many useful insights about forest ecosystems, using them to assess forest C balance ignores the fact that whole-tree growth is not directly analogous to diameter growth. Wood growth is measured in practice by changes in the diameter of a tree stem (DBH), and this radial growth provides the basis for a century's worth of growth and yield models. Models are necessary because changes in diameter are one-dimensional (e.g., linear), yet wood growth is a multidimensional process characterized by volume and wood density. As such, tree growth is best quantified by the mass of wood (e.g., the biomass) grown as a layer over the stem and branches (and roots) in a given year (Assmann, 1970). While changes in tree diameter are correlated with biomass increment, the relationship is not linear and is species-specific (Jenkins *et al.*, 2004). As a result, patterns in diameter growth, as measured from ring-widths (Fig. 1a), cannot accurately represent patterns of tree biomass growth (Fig. 1b) (LeBlanc, 1990; Visser, 1995). Trees whose growth appears identical in the single dimension of diameter, may actually be producing biomass at rates that differ by orders of magnitude, largely due to differences in stem geometry (i.e., the location of diameter increment on a stem of larger or smaller circumference), stature, and wood density (Fig. 1a, b). Further obscuring these differences, tree-ring data are often standardized to create dimensionless indices that correlate with climate parameters (Cook & Peters, 1997) subsequently hiding meaningful differences in biomass (Fig. 1c). These dimensional differences are real, and have significant implications for questions that depend on the absolute mass of wood growth. This distinction is important when we want to know how climate change will affect growth of competing tree species that differ in stature and impact the potential for C sequestration in forest wood.

A second factor that limits understanding of tree growth is the fact that tree-ring studies aimed at historical climate reconstruction use unrepresentative sampling designs that are not capable of producing area-based estimates of growth that are scalable to forests or landscapes (Brienen *et al.*, 2012; Nehrbass-Ahles *et al.*, 2014). Inference based on these data can overstate the strength of relationships between climate variation and aggregate growth. Sampling for historical reconstruction typically targets species and individual trees that are old, sensitive to annual climate, and free from competition (Fritts, 1976), thereby missing the variation in individual response that exists within a forest (Carrer, 2011). In contrast to the few sensitive trees suitable for climate reconstruction, the vast majority of trees grow in dense forest environments where they must compete intensely for light, growing space, and belowground resources (Clark *et al.*, 2012). In temperate
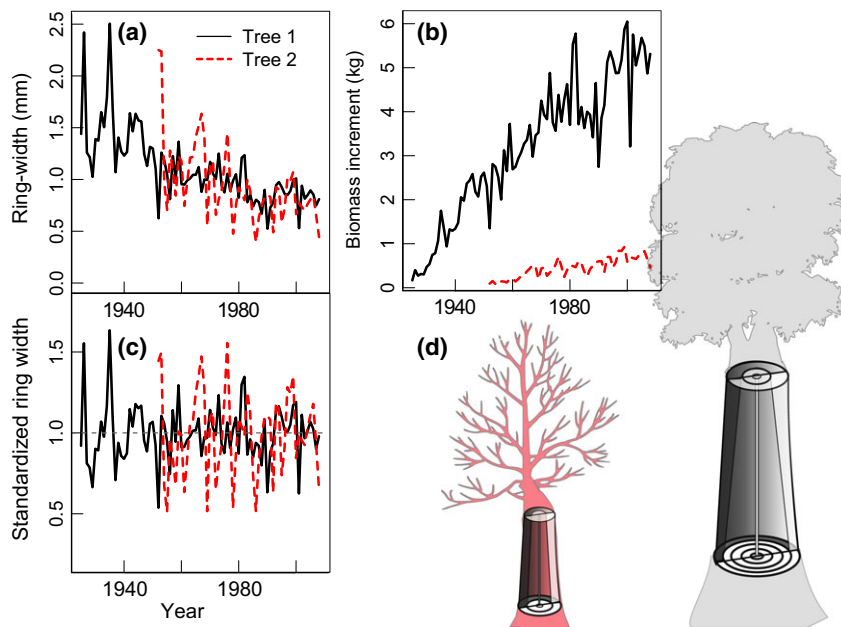
Fig. 1 Tree growth from a large *Quercus rubra* (tree 1) and small *Fraxinus nigra* (tree 2) illustrates different metrics of tree growth. Growth is measured in a single dimension by changes in diameter (ring-width) (a) which are roughly equivalent for these two trees, while growth in terms of biomass for the same trees (b) follows a significantly different pattern and illustrates large departures in absolute growth. Ring-width data are commonly standardized to unitless indices to relate to climate anomalies, which also obscures growth differences between trees (c). Two trees of different species, diameter and height (d) can have similar diameter growth (in terms of ring-width) that nonetheless corresponds to very different absolute growth in terms of wood mass and volume (a and b). The outer rings of these diagrammed trees, although equivalent in ring-width, have been shaded to highlight how stem geometry results in very different volume growth for trees of different stature. The specific tree records used in this example were selected to illustrate how the growth metrics RW and RWI do not capture differences in biomass growth. These examples are not intended to indicate mean differences in growth among species or across sites.

biomes where closed-canopy forest conditions dominate, climatic conditions may be less limiting to tree growth than these other factors (Canham & Thomas, 2010). Predicting how these forests respond to global change requires an understanding of how populations of forest species, not just idiosyncratic individuals, vary mass growth with climate. Sampled trees must be representative of populations growing in typical canopy environments to draw meaningful inferences about annual climate effects on population-level C uptake.

We outline these limitations explicitly because studies aimed at quantifying annual climate–tree growth relationships typically report analyses based on variation in dimensionless indices of radial growth, rather than mass-based models, or sometimes mistakenly conflate the two (Anderegg *et al.*, 2015). This body of research offers a wealth of information about the correlation of one-dimensional radial growth anomalies with various climatic parameters such as monthly or annual temperature and precipitation. However, analyses based on growth indices cannot quantify the relative impact of climate variation on individual tree

and forest biomass accumulation. As individual biomass growth generally increases with tree size (Stephenson *et al.*, 2014), we expect that forests with diverse tree sizes might experience more variation in C accumulation rates when large trees are climate-sensitive rather than small trees. Size matters, as do other structural characteristics of forests that can affect competition and growth. By considering climate, tree and stand factors simultaneously using mass-based models, we can begin to make inferences about how much wood growth, C accumulation, and the carbon cycle might be altered under a changing climate.

Here, we used an individual, that is, tree-level, hierarchical model to characterize to what extent whole-tree growth depends on climatic, tree, and stand structural variation. We estimate climatic effects on mass growth, measured from tree-ring reconstructions of aboveground biomass increment, while simultaneously estimating effects of individual tree structure (size and age) and stand competition. We tested three broad hypotheses asking: (i) whether structural or climatic covariates are stronger predictors of growth, (ii) whether tree growth varies across individuals in

response to climate and whether that variation eclipses interspecific differences, and (iii) whether climate responses vary based on historical species range. We standardized covariates of interest, allowing us to compare the magnitude of fitted coefficients to discern their relative effects on growth and included species-specific spatially structured latent covariates via the addition of a residual spatial process term.

We examine a representative sample including 15 tree species (Table 1) from a transition zone between temperate and boreal forest biomes in northern Minnesota, USA. This sample included four species at the cool northern edge of their historical range, four at their warm southern edge, and seven species closer to the center latitude of their range (Fig. S1). We hypothesized that annual climate variation in this transition zone would explain significant variation in growth, but that the magnitude of its effects would be smaller than variation explained by structural characteristics of the trees and forests in which they grow. We also hypothesized that individual trees would respond differently to climatic drivers. If there is widespread variation in individual response to climate within a species, aggregate growth among species may differ less than expected as the climate changes. We hypothesized that growth of species near their cool range margin would be more temperature-sensitive (Ettinger *et al.*, 2011), while spe-

cies at the southern edge of their range would be more sensitive to drought. We compared the posterior distributions of these climatic effects among species to evaluate which species are most vulnerable or resilient to predicted climate change.

Materials and methods

Study area

The Superior National Forest (47.8°N, 91.7°W) in Minnesota, USA, falls within the boreal–temperate forest ecotone where the historical distributions of cool-adapted boreal species overlap with the northern range margins of warm-adapted temperate species (Fig. S1). This forest transition zone is characterized by a continental climate with cold winters and short growing seasons. Annual temperatures across sample sites averaged 2.34 °C (SD = 0.37 °C) and annual precipitation averaged 684 mm (SD = 48 mm) from 1900 to 1970. These annual means increased to 3.03 °C (SD = 0.25 °C) and 734 mm (SD = 44 mm) in the period 1970–2010.

Aboveground biomass growth data from tree rings

We used growth data generated from tree increment cores that were collected in June through August of 2010. We sampled 36 forest stands representing eight common forest types in the temperate and boreal forest transition zone (Foster *et al.*, 2014). Within each stand, three 400 m^2 circular plots were measured for forest structural attributes. Every live overstory tree greater than 10 cm diameter at breast height (DBH) was mapped and cored at 1.3 m height for tree-ring analysis. Due to the large number of trees (3245), we extracted one core per tree. We processed and measured increment cores using a Velmex measuring stage and standard dendrochronological techniques (Holmes, 1983). We cross-dated tree-ring series to conspecific trees within the same stand or geographic neighborhood using the pointer year method (Yamaguchi, 1991) and confirmed dating using the program COFECHA (Holmes, 1983). Correlation among cross-dated series averaged 0.540 and ranged from 0.290–0.732 among trees in a series (Table S1) and autocorrelation was typically 1st or 2nd order.

We estimated whole-tree aboveground biomass in a given year by applying species-specific allometric equations (Table S3) to tree diameters that were reconstructed from the tree-ring series as described in Foster *et al.* (2014). The biomass increment (e.g., mass growth) for a given year was the difference between tree biomass in year *t* and the biomass in the previous year. When we use the terms biomass or biomass increment hereafter, we are referring to aboveground components. While the minimum size for the trees sampled in 2010 was 10 cm, the time series of reconstructed diameters covering the century prior to sampling resulted in a mean DBH for all observations of 9.8 cm (Table S2). Tree age could be reliably reconstructed when increment cores reached the pith, or very close to it (Appendix S2) (Foster *et al.*, 2014).

Table 1 Summary of observed tree biomass growth increment data (kg yr^{-1}) by species. Minimum observed growth for all species was 0 kg yr^{-1}. See Appendix S2 for details on data transformation. Standard deviations associated with the means are shown in parentheses

Species	Code	No. trees	No. tree years	Mean growth	Max growth
Abies balsamea	ABBA	365	13391	1.1 (0.9)	12.8
Acer rubrum	ACRU	87	5646	1.6 (1.8)	21.9
Acer saccharum	ACSA	175	12793	3.1 (3.5)	35.7
Betula papyrifera	BEPA	273	19682	1.8 (1.9)	24.3
Fraxinus nigra	FRNI	132	10374	0.8 (0.7)	5.2
Larix laricina	LALA	10	707	0.7 (0.7)	4.9
Pinus banksiana	PIBA	383	16137	2.6 (1.8)	17.4
Picea glauca	PIGL	96	4395	2.1 (2.3)	25.1
Picea mariana	PIMA	400	25971	1.3 (1.5)	28.6
Pinus resinosa	PIRE	33	1438	3.7 (3.4)	22.6
Pinus strobus	PIST	56	4243	2.6 (2.6)	19.1
Populus grandidentata	POGR	23	1723	2.9 (2.2)	14.5
Populus tremuloides	POTR	93	4466	4.4 (5.7)	66.1
Quercus rubra	QURU	118	7803	1.8 (1.5)	10.1
Thuja occidentalis	THOC	47	4876	1 (1.1)	8.5
ALL		2291	133645	1.9 (2.3)	66.1

Climate data

We extracted monthly maximum and minimum temperature and total precipitation for all tree-ring plot locations from the PRISM gridded climate dataset from 1895 to 2010 (Daly *et al.*, 2008). PRISM data have been spatially interpolated to 30-arcsec grid cells (~800 × 800 m) using relationships between climate and geographic factors such as elevation, location, coastal proximity, aspect, and orographic lift (Daly *et al.*, 2008). We calculated mean annual temperature (TEMP) from the prior October to the current September and an index of summer moisture stress for each site. We estimated monthly potential evapotranspiration (PET) using the Hargreaves & Samani (1982) approach, and then took the ratio of total precipitation to PET from June to August (P/PET), a common index of growing season moisture stress (Martínez-Vilalta *et al.*, 2011). P/PET is greater than one when precipitation exceeds PET, while values below one represent a moisture deficit. Across time and space, P/PET values for our study area averaged 0.902 and ranged from 0.331–1.90 (Table S2).

To interpret model results in the context of future climate change, we downloaded 1 degree bias-corrected and downscaled general circulation model (GCM) projections centered on our study area (47.5°N Latitude and 91.5°W Longitude) from the Coupled Model Intercomparison Project Phase 5 (CMIP5) (Maurer *et al.*, 2007) (http://gdo-dcp.ucllnl.org/downscaled_cmip5_projections/, accessed 2014-04-07). CMIP5 data contain climate model simulations for between 22 and 32 different GCMs and four forcing scenarios called representative concentration pathways (RCPs) (Moss *et al.*, 2010). We selected the radiative forcing trajectories RCP 4.5 (~4.5 W m^{-2} stabilized after 2100) and RCP 8.5 (~8.5 W m^{-2} in 2100) and used one ensemble member per GCM (randomly selected for GCMs with multiple runs) to construct ensemble means and quantiles of forecast outcomes. We calculated mean annual temperature and P/PET from CMIP5 ensemble means using the same approach applied to historical PRISM data.

Biomass growth models

We modeled tree growth (i.e., annual aboveground biomass increment) for 15 species as a function of tree and forest stand structure and climatic variability using a Bayesian framework. Differences in tree structure were quantified by tree size (reconstructed diameter at breast height, DBH) and tree age (measured from year of recruitment to 1.3 m height). We account for the changing competitive environment experienced by individual trees by incorporating the derivative of average stand biomass growth (DERIV) (Foster *et al.*, 2014) as a covariate. DERIV is the instantaneous slope of a 30-year spline fit to the stand-level sum of annual biomass growth. When DERIV is positive, stand growth is increasing into available growing space; when it is flat or negative, growing space is fully occupied or decreasing. We tested growth response to climatic variability with covariates for mean annual temperature (TEMP) and growing season moisture stress (P/PET) for the current and two preceding years, as well as the interaction TEMP x P/PET. We included lagged P/PET because tree growth is autocorrelated through time, partly because trees store photosyn-

thate from previous growing seasons as nonstructural carbohydrates to hedge against unfavorable years (Carbone *et al.*, 2013) and correlations were strongest in our tree-ring data for time lags up to 2 years. We note that by including tree size and age, we are fitting the 'growth-related trends' that are typically removed from tree-ring data via standardization (Cook & Peters, 1997). The difference in our approach is that we model these relationships as well as the residual climate response simultaneously, rather than relying on the more typical curve fitting approach used in dendroclimatology that is not informed by tree size (Cook & Peters, 1981).

Model specification

In addition to the stand and climate variables described above, we also want to account for unobserved variables that might influence growth at local scales (e.g., soil, competition, and disturbance) on individuals within a species. At a given tree location s we model the log of annual biomass growth increment $y_{t,j}(s_i)$ for tree i, observation t, and species j using the spatially varying linear regression model

$$y_{t,j}(s_i) = \alpha + \beta_j(s_i) + x_{t,j}(s_i)^\top \delta(s_i) + \epsilon_{t,j}(s_i), \qquad (1)$$

where α is the intercept, $\beta_j(s_i)$ is a species- and tree-specific spatial random effect that provides local adjustment (with structured dependence) to the mean, and the $p \times 1$ vectors $x_{t,j}(s_i)$ and $\delta_j(s_i)$ are time-specific covariates and associated slope parameters, respectively. Specifically, $x_{t,j}(s_i)$ comprises tree- and stand-level variables log(AGE), log(DBH) and DERIV, and climate variables TEMP, P/PET, (P/PET)$_{t-1}$, (P/PET)$_{t-2}$, and TEMP x (P/PET). $\epsilon_{t,j}(s_i)$ captures the tree-specific spatially uncorrelated error term. To facilitate comparison, all variables were scaled to have mean zero and variance of one (Gelman & Hill 2007).

We interpret the $\beta_j(s_i)$'s as capturing the effect of unmeasured or unobserved covariates with spatial structure that act on individuals of a given species. The intuition here is that we might expect local latent environmental effects on individual growth, but those effects may differ by species. Such spatially structured latent variables can be captured via a spatial Gaussian process (see, e.g., Banerjee *et al.*, 2014, page 55, for details on spatial Gaussian processes). Specifically, for a tree of species j at generic location s, we assume spatial random effects follow a zero-centered spatial Gaussian process, $\beta_j(s) \sim GP(0, C_j(\cdot; \theta_j))$, where the covariance function $C_j(s, s'; \theta_j) = \text{Cov}(\beta_j(s), \beta_j(s'))$ models the covariance corresponding to the pair of trees of species j at locations s and s'. The $n_j \times 1$ vector of process realizations, say $\beta_j = (\beta_j(s_1), \beta_j(s_2), \ldots, \beta_j(s_{nj}))^\top$, collected over all trees within the jth species follows a multivariate normal distribution $N(0, \Sigma(\theta_j))$ with n_j x n_j covariance matrix $\Sigma(\theta_j)$. The (l,k)-th element of $\Sigma(\theta_j)$ is given by $C_j(s_l, s_k; \theta_j) = \sigma_j^2 \rho(s_l, s_k; \phi_j)$, where σ_j^2 is the process variance and ρ is a valid spatial correlation function with decay parameter ϕ_j. For the subsequent analysis we use an exponential correlation function $\rho(s_l, s_k; \phi_j) = \exp(-\phi_j \| s_l - s_k \|)$ where $\| s_l - s_k \|$ is the Euclidean distance between locations s_l and s_k. From a geostatistical perspective, the σ_j^2's can be viewed as the partial-sills whereas measurement error variance, or nugget, is captured by the

spatially uncorrelated zero-centered $\varepsilon_{t,j}(s_i \sim N(0, \tau^2))$. We defined the effective spatial range of the posterior distributions of the $\beta_j(s_i)$'s as the distance at which correlation is 0.05, calculated as $-\log(0.05)/\phi_j$.

We complete the Bayesian specification by assigning prior distributions to each parameter. We give α and the elements of $\delta_j(s_i)$'s flat, that is, noninformative, priors. Variance parameters σ_j^2's and τ^2 are assumed to follow inverse-Gamma distributions with a shape hyperparameter of 2 and scale set based on exploratory analysis using species-specific models and variogram analysis of model residuals. We assume the spatial decay parameters ϕ's have Uniform prior distributions with support between the minimum and maximum distance between tree locations, which includes individuals of a species across all stands.

Parameter inference was based on posterior distributions that were sampled using Markov chain Monte Carlo (MCMC). Full conditional distributions were available for all model parameters with the exception of the spatial process parameters, which were sampled using a Metropolis–Hastings algorithm. Specifics about the MCMC sampling algorithm are provided in Appendix S1.

Our central interest is in the impact of covariates on individual tree-level and species-level biomass growth. In addition to plots of the individual and pooled posterior distributions of δ, we are interested in assessing the variability in regression coefficients at the individual level within species as well as their variability between species. We summarize these as:

$$V_{j,k}^{\text{within}} = \sum_{i=1}^{n_j}(\delta_{j,k}(s_i) - \bar{\delta}_{j,k})^2/(n_j - 1) \qquad (2)$$

and

$$V_k^{\text{between}} = \sum_{j=1}^{J}(\bar{\delta}_{j,k} - \bar{\bar{\delta}}_k)^2/(J - 1) \qquad (3)$$

for $k = 1,2...,p$ and $j = 1,2,...,J$, where p was previously defined as the number of covariates, J is the number of species, $\bar{\delta}_{j,k}$ is mean of the $\bar{\delta}_{j,k}(s_i)$'s over the n_j trees within the jth species for the kth regression coefficient, and $\bar{\bar{\delta}}_k$ is the mean over the J species $\bar{\delta}_{j,k}$'s.

We can generate samples from the posterior distributions of $V_{j,k}^{\text{within}}$ and V_k^{between} by calculating (2) and (3) for each post-burn-in MCMC sample of δ. We generate corresponding posterior distributions for the $\bar{\delta}_{j,k}$'s in a similar way.

Alternative models and model evaluation

Inference about covariate impact on individual tree vs. species variability requires tree-specific estimates of δ as specified in (1). However, from a predictive standpoint, it might be useful to assess the need for individual tree-level, or even species-level, regression coefficient estimates. Therefore, we consider two submodels of (1), first pooling over individuals within species

$$y_{t,j}(s_i) = \alpha + \beta_j(s_i) + x_{t,j}(s_i)^{\top}\delta_j + \epsilon_{t,j}(s_i), \qquad (4)$$

then over species,

$$y_{t,j}(s_i) = \alpha + \beta_j(s_i) + x_{t,j}(s_i)^{\top}\delta + \epsilon_{t,j}(s_i), \qquad (5)$$

We note the submodels maintain the species- and tree-specific spatial random effects, $\beta_j(s_i)$'s, on the model intercept to account for any spatially structured latent variable effects on individuals.

We assessed goodness-of-fit of the three candidate models with the deviance information criterion (DIC) (Spiegelhalter *et al.*, 2002), the predictive model choice criterion (D) (Gelfand & Ghosh, 1998; Equation 6), and a scoring rule (SR) defined in Gneiting & Raftery (2007, Equation 27). These criteria evaluate both the closeness of the mean predicted value to the observed data as well as the spread of the individual predictions around the observed data. All three criteria also penalize increasing model complexity and poor fit to observed data. For DIC the term p_D is considered the effective number of model parameters and for D the term P penalizes both under- and overfitted models. When comparing the candidate models, the preferred model will yield predictions with low variance that are, on average, close to the observed data while having low model complexity. Larger values of SR and lower values of DIC and D indicate a better fit to the data.

Parameter posterior inference and goodness-of-fit for each candidate model were based on 15 000 post-burn-in samples from 3 MCMC chains (5000 from each chain). Convergence was diagnosed using the CODA package in R (R Core Team 2013) by monitoring mixing of chains and the Gelman–Rubin statistic (Gelman & Rubin, 1992). Satisfactory convergence was diagnosed within 25 000 iterations for all parameters.

Results

Summary statistics

Annual tree-level biomass growth averaged 1.9 kg yr^{-1} across all 2291 trees and 15 species, and ranged from 0 to 66.1 kg yr^{-1} (Table 1). Average biomass growth of individual species ranged from 0.7 [0.64,0.74] and 0.8 [0.78,0.81] kg yr^{-1} in the slowest growing *Larix laricina* and *Fraxinus nigra* (95% CIs shown in brackets), to the highest mean growth of 3.1 [3.1,3.2], 3.7 [3.5,3.8], and 4.4 [4.2,4.6] kg yr^{-1} for *Acer saccharum*, *Pinus resinosa*, and *Populus tremuloides*, respectively. Most tree species were represented by >50 and up to 400 individual trees, although the least sampled species were only represented by 10–33 individuals (*L. laricina*, *P. resinosa*, and *P. grandidentata*).

Candidate models

Based on the goodness-of-fit metrics, the full model (Eqn 1) that allowed growth responses to vary by individual trees within species performed better than alternative models that pooled tree-level data within species (Eqn 4) or pooled data without regard to individuals or species (Eqn 5) (Table 2). The goodness-of-fit metrics

Table 2 Goodness-of-fit metrics for candidate models. The score that indicates improved fit is noted in bold

	Model(1) individual effects	Model(4) pooled effects (within species)	Model(5) pooled effects (all observations)
PD	18 739	1516	1414
DIC	**20 561**	55 432	66 719
P	9043	11 847	12 890
D	**15 870**	23 436	25 519
SR	**257 069**	193 107	181 536

DIC and D were minimized while the score SR was maximized with the full model (Table 2), indicating that fitting individual tree responses represented the data better even though it required estimation of a much larger parameter set. All subsequent results and discussion focus on the full model (1) that allowed individual tree responses.

Species-level growth response

Tree biomass growth increased with tree size for all species (Fig. 2a). Tree size affected growth more than any other covariate with a mean coefficient $\hat{\bar{\delta}}$ of ~1 (0.95) across species. The effect of age on biomass growth was also relatively large (Fig. 2b) and significant for all species. Age had negative coefficients in the model ($\hat{\bar{\delta}} = -0.61$). The mean trend in stand growth (DERIV) had a positive, although small ($\hat{\bar{\delta}} = 0.05$), effect on the growth of 8 of 15 species (Fig. 2c). This suggests that individuals in these species respond similarly to the competitive conditions reflected by the general growth trend of the stand. We expected shade-intolerant species that establish canopy dominance early in stand development to respond most strongly to stand-level competition. Similarly, we expected shade-tolerant species to show a range of both positive and negative growth responses to stand-level trends, under the assumption that they can withstand more variable
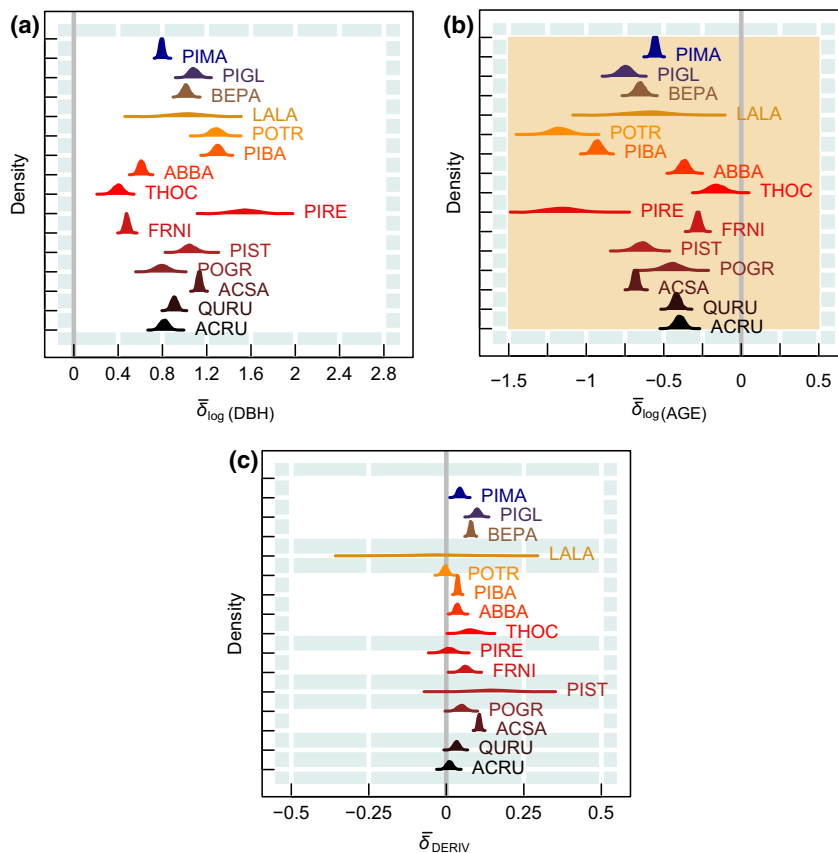

Fig. 2 Posterior distributions for regression parameters ($\bar{\bar{\delta}}$) associated with the tree and stand structure covariates tree size (DBH), age, and stand competition (DERIV). Species codes and names can be found in Table 1. Species are ordered based on the central latitude of their historical range, with northern species at the top and southern species at the bottom. Limits on x-axis vary among panels. Significant posterior distributions (97.5% > 0) are highlighted against a solid white background, while significant negative distributions were highlighted with a solid tan background. Nonsignificant distributions appear against the gridded gray background.

light conditions. Instead, half of the species with significant positive responses to aggregate growth trends are tolerant of shade: *Abies balsamea*, *Picea mariana*, *P. glauca*, and *Acer saccharum*. We note that most of the northern species responded positively to trends in stand growth, with the exception of *P. tremuloides*.

Annual climatic variation in terms of mean annual temperature and summer moisture stress affected growth in a variety of ways. Growth of five species responded significantly to a combination of current year TEMP and P/PET, characterized by negative coefficients on each covariate and a positive coefficient on the interaction term (Fig. 3). The significant interaction indicates that annual growth response to temperature depends on the growing season moisture stress, and *vice versa*. We interpreted this interaction by plotting growth in response to summer moisture stress for mean annual temperatures that range from the mean TEMP (2.8 °C) to up to ±2 SD (4.8 °C) (Fig. 6). Interaction plots show that growth decreases in response to increasing moisture availability in cooler than average years (blue lines), and growth increases with moisture availability in warmer than average years (red lines). Years with average annual temperatures show less of a growth response across the range of summer moisture stress (gray lines). Species with larger coefficients on these climate parameters, such as *P. grandidentata*, had a much larger overall growth response than species with smaller coefficients, such as *Q. rubra* (Fig. 6). Only three species did not show a directional biomass growth response to any climate variables: *Picea mariana*, *Pinus resinosa,* and *Thuja occidentalis*. The remaining species showed a significant response to growing season moisture availability from prior years. Significant coefficients on lagged P/PET tended to be positive for conditions 1 year prior to growth and negative for conditions 2 years prior to growth. *P. tremuloides* was unique in having a negative growth response to moisture availability of both prior years, and *A. saccharum* was the only species to respond positively to both. The magnitude of climatic effects on growth represented by standardized coefficients on the covariates was small (means from −0.05 to 0.05) relative to coefficients for tree size and age.

The species and tree location specific residual spatial structure captured by the $\beta_j(s_i)$'s represents autocorrelation in growth that is not explained by the climate, tree, or stand covariates used in the model. Posterior estimates of the effective spatial range of species-specific processes varied from approximately 10 to 40 m, with the means of most species centered between 15 and 25 m (Fig. 4). These differences in species effective spatial range and the process variance estimates, σ_j^2's

(Fig. S4), suggest individual trees are responding to unmeasured stresses or resources in species-specific ways. Two species with the broadest effective spatial ranges (Fig. 4), *P. tremuloides* and *A. balsamea*, are highly preferred hosts of the native defoliators, forest tent caterpillar (*Malacosoma disstria*) and spruce budworm (*Choristoneura fumiferana*), respectively. The wide range in their spatial dependence may reflect the variable patterns of these and other disturbances. Residual spatial patterns may also reflect indirect processes, such as synchronized release of nonhost species during insect outbreaks.

Variation in individual tree growth response

Individual, tree-level responses to the different structure and climate covariates varied (Figs 2, 3, and 5), and for some species, widely. For example, *B. papyrifera* responses to AGE and DBH were highly variable (Fig. S3), as was *Pinus strobus* response to the stand-level trend DERIV (Fig. S3), and responses of *P. resinosa*, *Populus tremuloides,* and *Larix laricina* to TEMP (Fig. 5). For other species, there was much less variation among individuals (i.e., trees all responded about the same to the different predictors as *F. nigra* did for TEMP (Fig. 5)). The cool-adapted, northern conifers *Abies balsamea*, *Picea mariana*, *P. glauca* and *Pinus banksiana* all had fairly narrow range of reactions to all the covariates (Fig. 5). Posterior distributions of variances defined in Eqns 2–3 (Figs 5 and S4) suggest variability among individual tree growth response to climate was larger than variability in response among species.

Relationship between climate response and geographic range

Within-species variance in individual response to TEMP or P/PET did not show a trend with the central Latitude of species ranges. There was, however, a significant negative trend between mean V^{within} and central Longitude of species range (where degrees west are represented by negative values) (V_{TEMP} trend = −0.001, $r^2 = 0.28$, $V_{P/PET}$ trend = −0.002, $r^2 = 0.29$). Boreal species whose historic ranges spanned a much greater east–west extent across Canada's boreal forest (Fig. S1) had higher variability in individual growth response to TEMP and P/PET than species whose central Longitude reflected ranges restricted primarily to eastern North America. Central Latitude and Longitude of species range was strongly, negatively correlated (trend = −0.46, $r^2 = 0.72$), suggesting that these geographic centroids are imperfect, if useful, proxies to characterize species climatic niche.
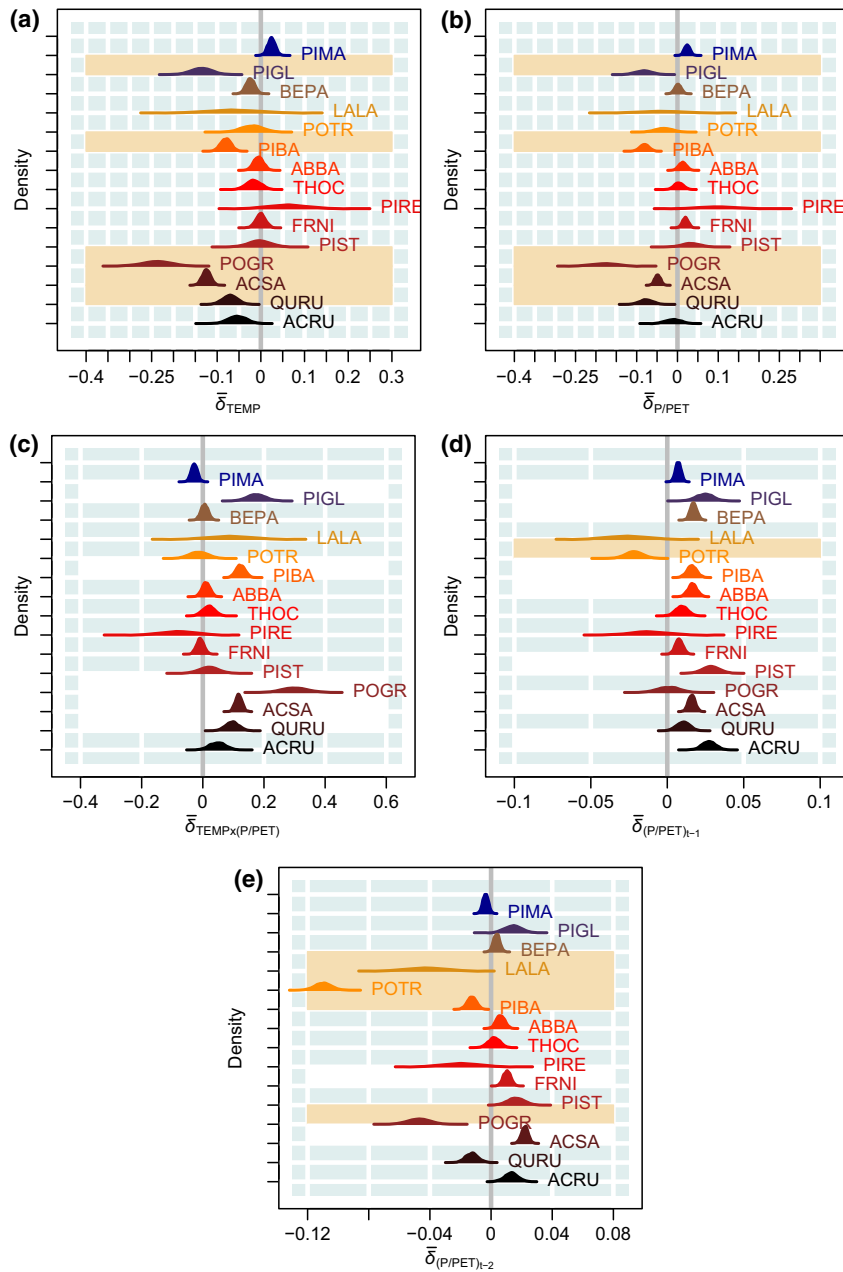
Fig. 3 Posterior distributions for regression parameters ($\bar{\bar{\delta}}$) associated with annual climate covariates. Climate covariates include mean annual temperature (TEMP) (a) and growing season moisture stress derived from the ratio of summer precipitation to potential evapotranspiration (P/PET) for the current year (b), their interaction (c), and up to 2 years prior (P/PET$_{t-2}$) (d, e). Species codes and names can be found in Table 1. The vertical order of species corresponds to the central latitude of their historical range, with northern species at the top and more southern species at the bottom. Limits on the *x*-axis vary among panels. Positively significant posterior distributions (97.5% > 0) are highlighted against a solid white background, while significant negative distributions are highlighted with a solid tan background. Nonsignificant distributions appear against the gridded gray background.

Discussion

Individual trees varied in their growth response to mean annual temperatures and summer moisture stress. The variation among individuals within a species appeared to be wider than mean differences among species. The amount that biomass growth varied in response to annual climate was much smaller than the amount it varied in response to differences in tree age and size. Tree size affected growth more than any other covariate with a mean coefficient $\hat{\bar{\delta}}$ of ~1 (0.95) across species. If you consider two trees, one of mean size throughout the
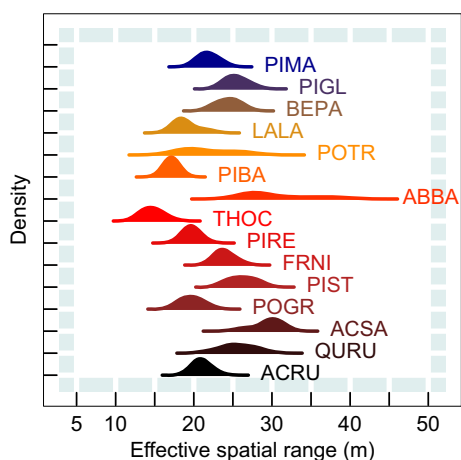
Fig. 4 Posterior distributions of the spatial process parameter effective spatial range that shows the distance over which latent spatial covariates are correlated. Species codes and names can be found in Table 1. All distributions differ significantly from zero.

growth series (DBH ~ 9.8 cm) and a tree one SD larger (+1.9 cm), these standardized coefficients mean that biomass growth of the larger tree should be greater by one SD, or about 4 kg yr^{-1} on average (Table S2). We are able to quantify these effects because we model biomass directly, which would not be possible if we modeled raw or detrended ring-width.

Age had negative coefficients in the model ($\hat{\bar{\delta}} = -0.61$), which could be interpreted to mean that biomass growth decreased with age. However, in multiple regression, covariation may influence the direction of each effect. Tree size and age are always intertwined. A tree cannot get bigger without also getting older, and one generally does not get older without getting larger (with some exceptions). When we predicted biomass growth from tree age alone using a univariate model, growth increased with age, as it did with size. When tree age was added to a model that included tree size, age acted as a correcting factor that accounts for inter-tree variation in growth rates that have accumulated over time. For two trees of the same size (~10 cm DBH), one that is 10 years old and another that is 20, the younger tree has grown twice as fast as the older one to reach the same size, which indicates that something about its genetics or local environment is favorable for growth. This information improves predictions of growth for each tree. By comparison, coefficients on climatic variables were generally smaller than |0.05|, meaning that their combined effects would only lower growth by ~0.2 SD (0.8 kg for an average tree), in warm and dry years (+1 SD TEMP, −1 SD P/PET). The importance of size and age to predict growth, relative to competition and climate, means that measuring or
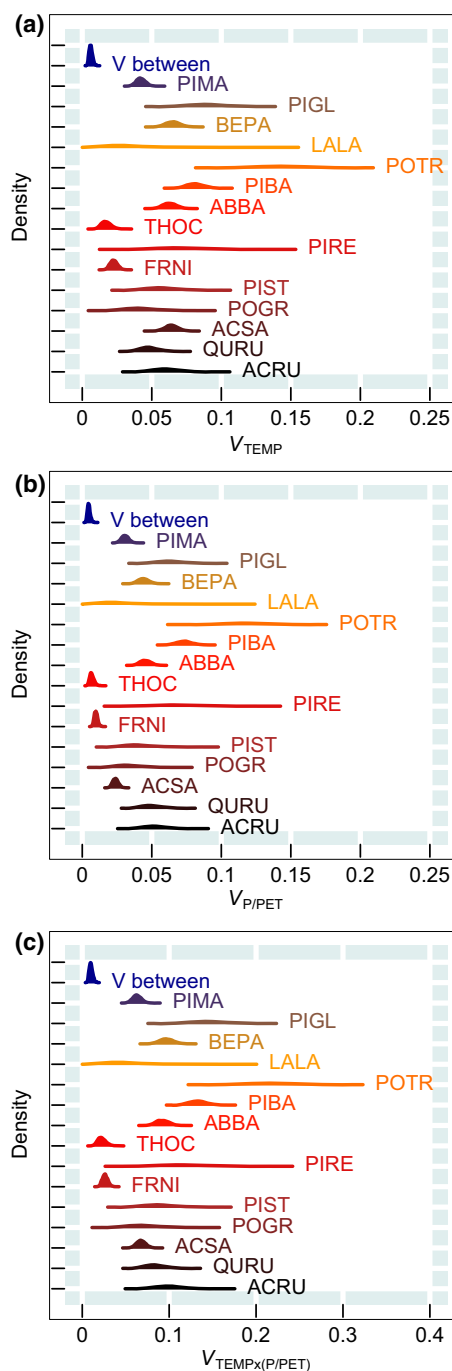

Fig. 5 Posterior distributions of within and between species variances of slope parameters (V) for three climate variables. Climate covariates include mean annual temperature (TEMP) (a), and growing season moisture stress derived from the ratio of summer precipitation to potential evapotranspiration (P/PET) for the current year (b), and their interaction (TEMP × P/PET) (c). Similar plots for the remaining covariates can be found in Fig. S3. Species codes and names can be found in Table 1.

predicting the physical structure of current and future forests could tell us more about C uptake rates through the year 2100 than growth responses related to climate change alone. The wide variability in individual tree responses further suggests that C uptake in mature forests may be buffered and resilient to a range of changes in climate (Fig. S2) that are projected for the boreal–temperate forest ecotone.

Comparing climate projections to the historical record experienced over the lifetime of the current population helps clarify whether climate impacts on growth will have biological significance for future competitive interactions (Fig. S2). Mean annual temperature is projected to increase in these forests from the historic long-term mean of 2.83 °C (1895–2011) to a mean of 6.43 °C 2055–2095 (Fig. S2), based on the mean of the CMIP5 ensemble of GCM simulations and the RCP 4.5 trajectory. A range of CMIP5 projections predict significant increases in TEMP by 2050, but nonsignificant changes in P/PET (Fig. S2). Years that were historically considered 'hot' (+2 SD) will occur more frequently. In the past, mean annual temperatures only exceeded +2 SD above the long-term mean (e.g., 4.81 °C) in 3 of 112 years (2.6%, 1895–2010), in 1931, 1987, and 1998. Climate projections from the CCSM4 GCM model and RCP 4.5 predict that mean annual temperatures will exceed 4.81 °C in 74% of years between 2010 and 2098. Based on historical response to warmer years (Figs 3 and 6), we expect growth of the temperate species *Q. rubra*, *A. saccharum*, and *P. grandidentata* and the boreal species *P. glauca* and *P. banksiana* to respond more strongly to summer moisture stress in the future, growing more in wet years, but even less in dry ones. We expect growth of the remaining species to be roughly the same as in the past, because individual variation includes both positive and negative responses to annual climate. Surprisingly, we find three temperate species growing at the northern edge of their range to be included among sensitive species that may suffer more under future droughts, although this prediction could be reversed if local precipitation is higher than current projections. The interaction of these climatic effects calls into question the simple assumption that temperate species like *A. saccharum* and *Q. rubra* will automatically have an advantage at the temperate–boreal ecotone under a changing climate (Reich *et al.*, 2015). At the same time, the projection that 74% of years over this century will be historically 'hot' years, compared to only 3% in the past, suggests that temperatures may exceed the local climate envelope to the extent that tree and species growth can no longer be predicted from past relationships.

Climate response did not vary with central latitude of species' historical ranges, but the within-species variation in response to TEMP and P/PET did vary sig-

nificantly with range longitude. This evidence suggests that boreal species whose ranges span the east–west extent of Canada express more individual variation in growth response to fluctuating annual climate than species whose ranges are restricted to the eastern half of North America. We expected that species growing at their range margins, whether warm or cool, would show more sensitivity to climate variation. Central latitude did not emerge as a strong proxy for species climatic niche, unlike recent studies examining effects on tree seedling productivity (Reich *et al.*, 2015). The importance of longitude on within-species variation likely reflects the east–west gradient in P/PET that ultimately grades into the prairie biome ~150 km from our study area (Danz *et al.*, 2013).
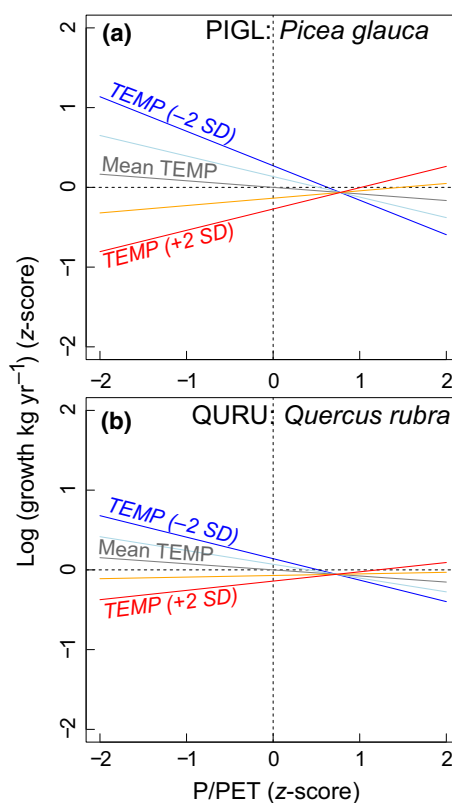

Fig. 6 Predicted growth across a gradient of standardized summer moisture stress (P/PET) under different mean annual temperatures (colored lines) demonstrates the effect of the significant interaction between these climate parameters. *P. glauca* shows a typical response (a), while *Q. rubra* has the narrowest response. Plots show predicted mean growth when all other covariates are at their mean value. Plots show that for average temperature years (solid gray lines), growth varies little in relation to growing season moisture stress. In extreme temperature years, growth responds strongly and in opposite directions to growing season moisture stress (blue and red lines). Other species showing this interactive response included *A. saccharum*, *P. banksiana*, and *P. grandidentata* (Fig. 3).

Implications for dendroecology

The size and age effects on tree growth would differ in magnitude if we had modeled relationships with tree ring-width or unitless ring-width indices (RWI) instead of biomass increment (Fig. S6). In particular, the negative effect of age would appear to be a stronger driver of growth than the positive effect of size if models predicted ring-width rather than biomass increment (Fig. S6), and the significance of species responses would differ for 12 species–covariate combinations (Figs 2 and 3). Models predicting RWI would differ from aboveground biomass models on the significance of 33 species–covariate relationships, and conclude that size does not predict growth for five species. Models that focus on basal area increment (BAI) or volume increment generally report growth effects for tree size and age that agree with ours (Cortini *et al.*, 2012; Michaletz *et al.*, 2015), namely a positive effect of size, accompanied by a negative effect of age, when both covariates are in a model (Martínez-Vilalta *et al.*, 2011). The creation of a residual ring-width chronology requires the imposition of a model that is intended to remove growth effects related to size and age (Cook & Peters, 1981). These residuals highlight the interannual variation in a ring-width time series, part of which is known to encode a climate-related signal. What gets lost in this process is the possibility that the climate signal may occupy an increasingly smaller percentage of biomass growth as trees get larger. This issue is frequently overlooked when dendrochronology data are relied on to inform projections of forest carbon balance (Anderegg *et al.*, 2015).

Our results suggest that research that relies on archived dendrochronology records, most of which have been sampled or processed in nonrepresentative ways, should exercise caution and resist inferring carbon cycle effects from variation in ring-widths (diameter increment) or standardized residual chronologies alone. When effects in tree rings imply an effect on forest C accumulation rates, those effects should be tested by converting the data to biomass, or at least BAI and testing how this transformation affects inference. In general, variation in linear measures of growth should not be conflated with the changes in biomass that drive the forest carbon cycle.

Sources of model uncertainty and directions for future work

Our models faced common sources of uncertainty that present a number of opportunities for future improvements to model design. One source of uncertainty arises from the allometric equations used to estimate aboveground biomass from reconstructed DBH. While we carefully selected biomass equations to be suitable to our sampled trees and study area (Table S3), allometric equations are often derived from limited sample sizes and may not include a wide range of tree diameters (Weiskittel *et al.*, 2015). Current efforts to sample and build new comprehensive allometric equations for North American tree species should provide opportunities to better characterize and minimize this source of uncertainty within a few years (Weiskittel *et al.*, 2015). Small sample sizes for three species, uncertainty around some age estimates, and unmeasured disturbances likely added uncertainty to some of our results. Finally, while we have argued that biomass increment is the best growth metric for inference relevant to C budgets, biomass models face challenges in predicting future and aggregate growth, mainly because DBH must be forecast as well to update the model.

Another significant challenge was presented by the need to characterize climate variation at scales local to individual trees using gridded climate data that have been interpolated at a coarser spatial resolution. The PRISM climate data imperfectly approximate actual climate variation experienced within each stand; thus, we would expect the climate responses to be stronger if a denser network of historical climate stations existed. The challenge of this scale mismatch has been discussed in prior work (Zhu *et al.*, 2014), and is an area of ongoing investigation, yet it would not be possible to assess differences in individual tree response without accepting some approximation in the climate data at this time.

Our analysis addresses one demographic process, variation in growth, and finds that individual variation overcomes many apparent differences in species-level response to changing annual climate. Yet to fully understand species vulnerability to climate change, we need models that also address demographic responses related to reproduction, establishment, and mortality (Clark *et al.*, 2012). Disturbances introduce noise that may mask climate–growth relationships and may change as temperatures rise leading to significant effects on growth and mortality. Disturbance changes and their effects on demographic rates are not directly addressed in our analysis. On the establishment side, observations from isolated, planted seedlings in climate warming experiments are increasingly being used to predict future, species-specific climate response and performance (e.g., Reich *et al.*, 2015); however, the importance of tree size, age, and competitive conditions in affecting within-species response in our models argues for caution in extrapolating these early trends given they only capture a single life stage and size class. As such, the use of models that simultaneously address these factors, such as those presented in this

and other work (Clark et al., 2013) may provide a more accurate portrayal of future species performance and ecosystem-level C dynamics. Future modeling efforts should aim to incorporate more of these processes simultaneously, which should become possible as remeasurement of extensive forest inventory plots continues (Vanderwel & Purves, 2014; Zhang et al., 2015). A recent analysis from remeasured forest plot data also found that stand structure, represented by total basal area, was a more important predictor of aggregate stand growth, recruitment and mortality than climate (Zhang et al., 2015). While the similarity between our findings suggests consistent results across studies, our data and modeling frameworks are different. In particular, our models capture annual variation in climate, which must be smoothed out over remeasurement periods of 5–10 years for inventory data (Zhang et al., 2015), and we account for multiple effects simultaneously.

In this study, we quantified for the first time how tree size and age affect annual biomass growth relative to climate response, and found that individual tree size and age were much more important when predicting growth rates than climate parameters. We propose that research related to understanding the potential for C sequestration in forests should be prioritized based on this result. Prediction of future C uptake rates in temperate forests will benefit most by (i) improving measurement of current tree demographic rates, particularly related to mortality and establishment, then (ii) improving our ability to estimate the size, age and species composition of current and future forests, and (iii) improving our ability to predict tree growth response to annual climate variation. Future efforts should account for variation in climate response among individuals using representative sampling designs, and consider how interacting responses to temperature and moisture stress may challenge our expectations. The wide range of individual growth responses observed here suggests that aggregate growth and C uptake in mature forests may be more resilient to climate change than expected in the coming decades, although it remains to be seen whether threshold dynamics will push tree growth into unpredictable territory.

Acknowledgments

References

Anderegg WRL, Schwalm C, Biondi F et al. (2015) Pervasive drought legacies in forest ecosystems and their implications for carbon cycle models. Science, 349, 528–532.

Assmann E (1970) The Principles of Forest Yield Study. Pergamon Press, Oxford.

Banerjee S, Carlin BP, Gelfand AE (2014) Hierarchical Modeling and Analysis for Spatial Data, 2nd Edn. Chapman & Hall/CRC Monographs on Statistics & Applied Probability, 135, Taylor & Francis Group, Boca Raton, FL.

Brienen RJW, Gloor E, Zuidema PA (2012) Detecting evidence for CO_2 fertilization from tree ring studies: the potential role of sampling biases. Global Biogeochemical Cycles, 26, GB1025.

Canham CD, Thomas Q (2010) Frequency, not relative abundance, of temperate tree species varies along climate gradients in eastern North America. Ecology, 91, 3433–3440.

Carbone MS, Czimczik CI, Keenan TF, Murakami PF, Pederson N, Schaberg PG, Richardson AD (2013) Age, allocation and availability of nonstructural carbon in mature red maple trees. New Phytologist, 200, 1145–1155.

Carrer M (2011) Individualistic and time-varying tree-ring growth to climate sensitivity. PLoS ONE, 6, e22813.

Chu C, Bartlett M, Wang Y, Fangliang H, Weiner J, Chave J, Sack L (2015) Does climate directly influence NPP globally? Global Change Biology, 22, 12–24. doi:10.1111/gcb.13079.

Clark JS, Bell DM, Kwit M, Stine A, Vierra B, Zhu K (2012) Individual-scale inference to anticipate climate-change vulnerability of biodiversity. Philosophical Transactions of the Royal Society B, 367, 236–246.

Clark JS, Gelfand AE, Woodall CW, Zhu K (2013) More than the sum of the parts: forest climate response from joint species distribution models. Ecological Applications, 24, 990–999.

Cook ER, Peters K (1981) The smoothing spline: a new approach to standardizing forest interior tree-ring width series for dendroclimatic studies. Tree-ring Bulletin, 41, 45–53.

Cook ER, Peters K (1997) Calculating unbiased tree-ring indices for the study of climatic and environmental change. The Holocene, 7, 361–370.

Cortini F, Comeau PG, Bokalo M (2012) Trembling aspen competition and climate effects on white spruce growth in boreal mixtures of Western Canada. Forest Ecology and Management, 277, 67–73.

Daly C, Halbleib M, Smith JI et al. (2008) Physiographically sensitive mapping of climatological temperature and precipitation across the conterminous United States. International Journal of Climatology, 28, 2031–2064.

Danz NP, Frelich LE, Reich PB, Niemi GJ (2013) Do vegetation boundaries display smooth or abrupt spatial transitions along environmental gradients? Evidence from the prairie–forest biome boundary of historic Minnesota, USA. Journal of Vegetation Science, 24, 1129–1140.

Ettinger AK, Ford KR, HilleRisLambers J (2011) Climate determines upper, but not lower, altitudinal range limits of Pacific Northwest conifers. Ecology, 92, 1323–1331.

Foster JR, D'Amato AW (2015) Montane forest ecotones moved downslope in northeastern US in spite of warming between 1984 and 2011. Global Change Biology, 21, 4497–4507.

Foster JR, D'Amato AW, Bradford JB (2014) Looking for age-related growth decline in natural forests: unexpected biomass patterns from tree rings and simulated mortality. Oecologia, 175, 363–374.

Fritts HC (1976) Tree Rings and Climate. Academic Press, London.

Gelfand AE, Ghosh SK (1998) Model choice: a minimum posterior predictive loss approach. *Biometrika*, **85**, 1–11.

Gelman A, Hill J (2007) *Data Analysis Using Regression and Multilevel/Hierarchical Models*. Cambridge University Press, New York, NY.

Gelman A, Rubin DB (1992) Inference from iterative simulation using multiple sequences. *Statistical Science*, **7**, 457–472.

Gneiting T, Raftery AE (2007) Strictly proper scoring rules, prediction, and estimation. *Journal of the American Statistical Association*, **102**, 359–378.

Hargreaves GH, Samani ZA (1982) Estimating potential evapotranspiration. *Journal of the Irrigation and Drainage Division*, **108**, 225–230.

Holmes RL (1983) Computer-assisted quality control in tree-ring dating and measurement. *Tree-Ring Bulletin*, **43**, 69–78.

Iverson LR, Prasad AM (1998) Predicting abundance of 80 tree species following climate change in the eastern United States. *Ecological Monographs*, **68**, 465–485.

Jenkins JC, Chojnacky DC, Heath LS *et al.* (2004) Comprehensive database of diameter-based biomass regressions for North American tree species. Gen. Tech. Rep. NE-319. Newtown Square, PA: U.S. Department of Agriculture, Forest Service, Northeastern Research Station. 45 p.

Landscape Change Research Group (2014) *Climate Change Atlas*. Northern Research Station, U.S. Forest Service, Delaware, OH. Available at: http://www.nrs.fs.fed.us/atlas (accessed 28 February 2015).

LeBlanc DC (1990) Relationships between breast-height and whole-stem growth indices for red spruce on Whiteface Mountain, New York. *Canadian Journal of Forest Research*, **20**, 1399–1407.

Little EL (1971) *Atlas of United States Trees: Vol. 1. Conifers and Important Hardwoods*. US Department of Agriculture Miscellaneous Publication 1146, Washington, DC.

Martínez-Vilalta J, Lopez BC, Loepfe L, Lloret F (2011) Stand- and tree-level determinants of the drought response of Scots pine radial growth. *Oecologia*, **168**, 877–888.

Maurer EP, Brekke L, Pruitt T, Duffy PB (2007) Fine-resolution climate projections enhance regional climate change impact studies. *Eos Transactions AGU*, **88**, 504.

Michaletz ST, Cheng D, Kerkhoff AJ, Enquist BJ (2015) Convergence of terrestrial plant production across global climate gradients. *Nature*, **512**, 39–52.

Moss RH, Edmonds JA, Hibbard KA *et al.* (2010) The next generation of scenarios for climate change research and assessment. *Nature*, **463**, 747–756.

Nehrbass-Ahles C, Babst F, Klesse S *et al.* (2014) The influence of sampling design on tree-ring-based quantification of forest growth. *Global Change Biology*, **20**, 2867–2885.

Pan Y, Birdsey RA, Fang JY *et al.* (2011) A large and persistent carbon sink in the world's forests. *Science*, **333**, 988–993.

R Core Team (2013). *R: A Language and Environment for Statistical Computing*. R Foundation for Statistical Computing, Vienna, Austria. Available at: URL http://www.R-project.org/ (accessed 10 September 2014).

Reich PB, Sendall KM, Rice K, Rich RL, Stefanski A, Hobbie SE, Montgomery RA (2015) Geographic range predicts photosynthetic and growth response to warming in co-occurring tree species. *Nature Climate Change*, **5**, 148–152.

Spiegelhalter DJ, Best NG, Carlin BR, van der Linde A (2002) Bayesian measures of model complexity and fit. *Journal of the Royal Statistical Society Series B-Statistical Methodology*, **64**, 583–616.

Stephenson NL, Das AJ, Condit R *et al.* (2014) Rate of tree carbon accumulation increases continuously with tree size. *Nature*, **507**, 90–93.

Thomas SC, Malczewski G (2007) Wood carbon content of tree species in Eastern China: interspecific variability and the importance of the volatile fraction. *Journal of Environmental Management*, **85**, 659–662.

Vanderwel MC, Purves DW (2014) How do disturbances and environmental heterogeneity affect the pace of forest distribution shifts under climate change? *Ecography*, **37**, 10–20.

Visser H (1995) Note on the relation between ring widths and basal area increments. *Forest Science*, **41**, 297–304.

Weiskittel AR, MacFarlane DW, Radtke PJ *et al.* (2015) A call to improve methods for estimating tree biomass for regional and national assessments. *Journal of Forestry*, **113**, 414–424.

Yamaguchi DK (1991) A simple method for cross-dating increment cores from living trees. *Canadian Journal of Forest Research*, **21**, 414–416.

Zhang J, Huang S, Fangliang H (2015) Half-century evidence from western Canada shows forest dynamics are primarily driven by competition followed by climate. *Proceedings of the National Academy of Sciences of the United States of Americas*, **112**, 4009–4014.

Zhu K, Woodall CW, Clark JS (2012) Failure to migrate: lack of tree range expansion in response to climate change. *Global Change Biology*, **18**, 1042–1052.

Zhu K, Woodall CW, Ghosh S *et al.* (2014) Dual impacts of climate change: forest migration and turnover through life history. *Global Change Biology*, **20**, 251–264.

Supporting Information

Additional Supporting Information may be found in the online version of this article:

Table S1. Descriptive statistics from cross-dated tree-ring datasets.

Table S2. Covariate means and standard deviations across tree-ring data.

Table S3. Biomass allometric equations: references and DBH limits.

Figure S1. Overlap of historical species' ranges as mapped by Little (1971).

Figure S2. GCM projections of CMIP5 ensemble means and ranges for the study area.

Figure S3. Plots of individual variation metrics (V) within and among species.

Figure S4 Spatial process variance estimates (σ_j^2's) among species.

Figure S5. Examples of observed and predicted biomass growth.

Figure S6. Barplots of coefficient means by covariate.

Appendix S1. Model (1) MCMC sampling algorithm.

Appendix S2. Additional details on data preparation and transformation.